HEXAGONAL MESOPOROUS TITANOSILICATES AS SUPPORT FOR VANADIUM OXIDE – PROMISING CATALYSTS FOR THE OXIDATIVE DEHYDROGENATION OF *n*-BUTANE

Michal Setnička[1], Pavel Čičmanec[1], Roman Bulánek[1], Arnošt Zukal[2] and Jakub Pastva[2]

[1] Department of Physical Chemistry, University of Pardubice, Studentská 573, CZ532 10 Pardubice, Czech Republic, e-mail: michal.setnicka@upce.cz , Tel: +420 46 603 73 45, Fax: +420 46 603 70 68

[2] J. Heyrovský Institute of Physical Chemistry Academy of Sciences of the Czech Republic, v.v.i., Dolejškova 2155/3, CZ182 23 Prague 8

Abstract

The comparative study of structural properties and catalytic performance of V-containing high-surface mesoporous silica and mesoporous titanosilicate materials (HMS, Ti-HMS) in oxidative dehydrogenation of *n*-butane (C_4-ODH) was carried out. The aim of the study was to investigate effect of different titanium amount incorporated into silica support on the texture, speciation of vanadium complexes and its impact on catalytic performance. Prepared catalysts were characterized by XRF for determination of vanadium content, DTA/TG for thermal stability of matrix, XRD, SEM and N_2-adsorption for study of morphology and texture, FT-IR and DR UV-vis spectroscopy for verification of successful incorporation of Ti to the matrix and H_2-TPR and DR UV-vis spectroscopy for determination of vanadium complex speciation. All prepared materials were tested in *n*-butane ODH reaction at 460 °C. We conclude that titanium was successfully incorporated into mesoporous structure, which was preserved at least up to 600 °C. Catalytic activities of V-Ti-HMS catalysts were approximately four times higher than activity of V-HMS catalyst in spite of the fact that all samples exhibit the same amount of vanadium species with similar distribution. The selectivity to desired products was comparable for all catalysts. Enhanced catalytic activity of V-Ti-HMS materials allows activating of *n*-butane at significantly lower temperature (by 100 °C) compare with V-HMS materials.

Keywords: mesoporous titanosilicate, hexagonal mesoporous structure, vanadium, oxidative dehydrogenation, butenes

Highlights

- One-pot synthesis of mesoporous titano-silicates with HMS structure
- Titanium distribution in HMS support comparable to distribution in TS-1 material
- Long-time thermal stability of V-Ti-HMS catalysts under reaction conditions
- Four time higher yield to C4-alkene on V-Ti-HMS compare to V-HMS catalysts

1 Introduction

The great challenge of current chemical industry is functionalization of cheap and abundant C_2-C_4 alkanes from crude oil to corresponding olefins. For example, the oxidative dehydrogenation (ODH) of light alkanes can be used for production of alkenes instead of classically used dehydrogenation (DH) requiring very high temperatures (high energy consumption) at which additional coking and deactivation of catalyst normally occur [1-4].

Vanadium oxides are powerful redox catalysts in many industrial processes and they are taken as catalysts in oxidation reactions as well as for ODH [5-6].. However, they can not be used in its bulk form (it leads to nonselective reactions) [4] but have to be used as the well dispersed VO_X species anchored on the suitable support [2, 4, 7-9]. Activity and selectivity of these catalysts strongly depend on the degree of vanadium species dispersion [3, 5, 10-11], method of catalyst preparation [3, 10-11] and also the type of support has a dramatic effect [4, 7, 11-12]. Suitable supports for anchoring active species are mesoporous molecular sieves not only due to their peculiar textural properties but also due to the possibility of various modifications including different structural types and as well as different chemical compositions [13].

A large number of reviews [2, 4, 7, 14-16] and papers dealing with the ODH of light alkanes over vanadium supported materials have been published since 1990s and most of them used different structure of silica materials (e.g. silicalite [11] or mesoporous MCM-41[17-18], SBA-15 [9, 19-22], SBA-16 [9] and HMS [3, 10, 23-24]). The main advantages of silica mesoporous materials are: larger surface area (a good dispersion of active particles), thermal and hydrothermal stability and good mechanical properties [3, 25-26]. Next advantage of catalysts anchored on silica support (compared with Al_2O_3, TiO_2, ZrO_2 etc.) is that catalysts using silica supports are more selective to desired products [27-29]. However, they exhibit relatively low activity and C_4-ODH productivity due to high apparent activation energy of C-H bonds [27, 30]. The highest activities and sufficient selectivity in ODH reaction were attained using VO_X species supported on TiO_2 (anatase) surface, which allows to carry out the reaction at lower temperatures [8, 11, 28, 31-32]. Nevertheless, pure TiO_2 support has also some drawbacks, such as a relatively low specific surface area, which can be further reduced by sintering as a consequence of thermal treatments. Low surface area prevents dispersion of vanadium oxide species, which leads to the further decrease in selectivity [3, 11, 31-32]. These drawbacks prevent the use of TiO_2 as conventional support

for catalysts. One possibility how to solve this problem is to prepare a mixed Si-Ti support which combines suitable properties of both above mentioned SiO_2 and TiO_2 supports, respectively.

Previous studies showed that coating of silica support with anatase phase (impregnation or grafting by titanium alkoxide) as one of the frequent method for preparing TiO_2/SiO_2 [1, 31], TiO_2/MCM-41 [28, 32-33] and TiO_2/SBA-15 [27, 34] support. In this case it was obtined thermostable support with high specific surface (silica) and with good catalytic performance (TiO_2). These materials were doped by vanadium and obtained materials were studied in C_2-ODH [31, 35], C_3-ODH [1, 27, 31] and only in one case in C_4-ODH [11] reaction. The disadvantage of materials prepared in this way is their complicated synthesis with multiple synthesis and calcination steps. Moreover, these postsynthetic methods sometimes lead to the blocking of the channels by the formation of bulk metal oxide clusters [36]. To avoid these problems, several attempts have been made to incorporate titanium into the silica framework directly. This problem could be overcome using direct synthesis method as was published previously for Ti-SBA-15 [37-38], Ti-HMS [37, 39-41], MCM-41 [33, 40, 42] and MCM-48 [43] but according to our knowledge these materials were not prepared in titanium content higher than 9 wt.% [44].

In the present paper we report on one-pot synthesis of Ti-HMS support with high content of titanium. In this case we obtain hexagonal mesoporous silica support with the isomorphously exchanged titanium oxide species and they serve as an “anchor” for vanadium active species. The reason for this behavior is the difference in the isoelectric point of TiO_2 (IEP = 6-6.4) and SiO_2 (IEP = 1-2) supports. The acidic vanadium oxide species (IEP = 1.4) are preferentially bonded to the more basic TiO_2 [7]. Moreover, acid/base properties of Ti species in the support influence the basicity of the bridging oxygen in sup-O-V (sup = Si, Al, Ti, etc.) and therefore their reactivity [6, 27]. The part of the surface composed of silica positively affects selectivity to desired ODH products. We prepared three HMS support with different content of titanium (0, 6 and 19 wt.% respectively). These materials were investigated by DTA/TG, FT-IR, N_2-BET, SEM, XRD and DR UV-vis spectroscopy for the physico-chemical characterization of the mesoporous support structure. After impregnation of these matrices by vanadium we verified preservation of mesoporous structure. We used DR UV-vis spectroscopy and H_2-TPR for investigation of vanadium dispersion and for the study of catalytic activity we used ODH of *n*-butane which is interesting for the industry as well as very suitable reaction model at the same time [3, 11].

2 Experimental

2.1 *Catalysts preparation*

The hexagonal mesoporous silica (HMS) and hexagonal mesoporous titanosilica (Ti-HMS), were synthesized under ambient conditions according to the procedure reported by Tanev and Pinnavaia [45] with their modification for Ti-HMS. In a typical preparation, dodecylamine (DDA, Aldrich) as a neutral structure directing agent was added to the mixture of ethanol and re-distilled water. After 20 minutes of homogenization tetraethylorthosilicate (TEOS, Aldrich) was added as silica precursor in the case of HMS preparation or TEOS and tetraethylorthotitanate (TEOT, Aldrich) as a titanium precursor was added simultaneously in the case of Ti-HMS preparation. The reaction mixture was stirred at room temperature for 18 h. The solid product was filtered, washed by ethanol and calcined in air at 450°C for 20 h (with heating rate 1°C/min) for the template removal.

The vanadium oxo-species (1.5 wt.% of V) were introduced onto the support by the wet impregnation method from EtOH solution of vanadyl acetylacetonate. Impregnated samples were dried at 120 °C in air overnight and then calcined at 600 °C in air for 8 h (with heating rate 5°C/min).

The investigated samples were denoted as *x*Ti-HMS, where *x* is the titanium content in support in the weight percentage. V-*x*Ti-HMS is used for materials after impregnation of vanadium.

2.2 *Catalysts characterization*

The content of titanium was determined by means of ICP-OES by Integra XL 2 (GBC Dandenog, Australia) for both prepared Ti-HMS supports. The vanadium content was determined by means of ED XRF by ElvaX (Elvatech, Ukraine) equipped with Pd anode [46]. Samples were measured against the model samples (a mechanical mixture pure SiO_2 and $NaVO_3$) granulated to the same size as catalysts.

The structure and crystallinity of catalysts were probed by scanning electron microscopy (SEM) using JSM-5500LV microscope (JEOL, Japan) and by X-ray diffraction (D8-Advance diffractometer, Bruker AXE, Germany) in the 2θ range of 2-35° with Cu Kα radiation (λ = 1.5406 Å).

Specific surface area and texture of investigated samples were measured by means of nitrogen adsorption/desorption at temperature of liquid nitrogen for verification of mesoporous structure by using ASAP 2020 equipment (Micromeritics, USA). Prior to

adsorption isotherm measurement, the samples were degassed at 300 °C under turbomolecular pump vacuum for 8 hours. The specific surface area was calculated according to BET method. The mesopore volume was determined by DFT by using of "N2 @ 77K" model for cylindrical pores and oxide surface.

Thermal stability of prepared matrix was studied using Jupiter STA 449C (Netzsch, Germany) thermobalance. Around 40-50 mg of matrix were heated in corundum TG-DTA-crucibles under a flow of air at a heating rate of 10 °C/min up to 1200 °C and the α-Al_2O_3 was used as a reference material.

For verification of successful incorporation of titanium to the HMS matrix the infrared spectra were collected on Nicolet 6700 FTIR spectrometer equipped with DTGS detector. Samples were diluted using dry KBr, pressed into pellets and scanned in the range 1400-400 cm^{-1} with a resolution of 2 cm^{-1} (32 scans). The spectrum of blank KBr pellet was also measured to allow background subtraction.

The UV-vis diffuse reflectance spectra of dehydrated diluted samples were measured by using Cintra 303 spectrometer (GBC Scientific Equipment, Australia) equipped with a Spectralon-coated integrating sphere using a Spectralon coated discs as a standard. The spectra were recorded in the range of the wavelength 190-850 nm. The samples were diluted by the pure silica (Fumed silica, Aldrich) in the ratio 1:100 for avoid spectra detection limits overflow and to give better resolution of individual bands. All samples were granulated and sieved to fraction of size 0.25-0.5 mm, dehydrated before the spectra measurement and oxidized in the glass apparatus under static oxygen atmosphere in two steps: 120 °C for 30 min and 450 °C for 60 min and subsequently cooled down to 250 °C and evacuated for 30 min. After the evacuation the samples were transferred into the quartz optical cuvette 5 mm thick and sealed under vacuum. Additional details about diluting and measuring can be seen in ref. [47-48]. The obtained reflectance spectra were transformed into the dependencies of Kubelka-Munk function $F(R_\infty)$ on the absorption energy hν using the equation :

$$F(R_\infty) = \frac{(1 - R_\infty)^2}{2R_\infty} \quad (1)$$

where R_∞ is the measured diffuse reflectance from a semi-infinite layer [49].

Hydrogen temperature programmed reduction (H_2-TPR) was used for the study of redox properties and AutoChem 2920 (Micromeritics, USA) was used for the measuring. A 100 mg sample in a quartz U-tube micro reactor was oxidized in oxygen flow at 450°C

(for 2 hours). The reduction was carried out from 35 °C to 850 °C with a temperature gradient of 10 °C/min in flow of reducing gas (5 vol.% H_2 in Ar). The changes in hydrog n concentration were monitored by online connected TCD detector.

2.3 *Catalytic tests*

The *n*-butane ODH reaction was carried out in a glass plug-flow fixed-bed reactor at atmospheric pressure in the kinetic region (independently checked) and under steady stat conditions of reaction. Typically 400 mg of catalyst (grains 0.25–0.50 mm) was diluted with 3 cm^3 inert SiC to avoid the catalytic bed overheating. The catalysts were pre-treated in th oxygen flow at 450 °C for 2 hours before each reaction run. The input feed composition wa $C_4H_{10}/O_2/He$ = 10/10/80 vol.% - with a total flow rate of 100 cm^3 min^{-1} STP. The catalytic activity was measured at 460 °C under the steady state conditions. The analysis of reaction mixture composition was made by on-line gas-chromatograph CHROM-5 (Laboratorní přístroje Praha) equipped with thermal conductivity detector (TCD) and flame ionization detector (FID). The *n*-butane and products of ODH reaction (butadiene, 1-butene, *cis*-2-butene, *trans*-2-butene, propene and propane) were separated using a packed column with *n*-octane on ResSil (Restek) at 20 °C. The packed column Porapak Q (Supelco) was used for th analysis of ethane, ethene and CO_2. The molecular sieve 13 X (Supelco) was used for th separation of permanent gases (O_2, CO and traces of N_2). For details about calculation conversion, selectivity, yield and productivity please see our previous work [3].

3 Results and discussion

3.1 *Characterization of materials*

SEM images of prepared supports (Fig. 1) show poorly defined morphology of every studied sample. Particles exhibit uneven shapes of sub-micrometer size. Size of particles of Ti-HMS supports is significantly (approximately three-times) smaller than particles of pur silica HMS support. Similar observation has been described by Comite *at al.* [1] who prepared TiO_2/SiO_2 support by grafting and they assign this behaviour to modification in calcination step. SEM-EDX mapping of Ti content led to the conclusion that Ti is spread homogeneously in all parts of support and no TiO_2 clusters were detected. Moreover mapping of vanadium content in the catalysts prepared by impregnation of supports shows that vanadium is distributed uniformly in all parts of catalysts and no V_2O_5 clusters and typical orthorhombic needles were observed in any sample (not shown here).

XRD patterns of supports and catalysts show (see Figure 2) characteristic broad low-angle diffraction peak at $2\theta = 2 - 2.5°$ attributable to a d_{100} diffraction typical for hexagonal lattice structure of mesoporous materials [40, 45]. The value of d_{100} spacing slightly changed for individual support in the range from 3.3 to 3.9 nm in correspondence with literature [42, 50]. This result corresponds to the changes in pore size distribution obtained from N_2 adsorption/desorption isotherm NLDFT analysis (see inset in Fig. 3). In addition, very broad peak with low intensity among 15-35 ° was detected in the X-ray powder patterns of all samples. This signal is usually assigned to the presence of amorphous SiO_2 wall [51-52]. Similar patterns were reported for hexagonal mesoporous materials in literature [10, 40-42, 50, 53]. Absence of diffraction lines belongs to TiO_2 (anatase and/or rutile) crystallites or V_2O_5 crystallites in the XRD patterns of all supports and catalysts confirm results from SEM; titanium is incorporated into HMS framework and do not form separated crystallites of TiO_2 and vanadium species are finely spread on the surface of supports without creation of oxide-like clusters or separated V_2O_5 crystallites.

BET specific surface area of parent materials and catalysts are summarized in Table 1. S_{BET} of parent supports slightly decreases with increasing content of titanium and ranges from 880 $m^2\ g^{-1}$ for pure HMS to 800 $m^2\ g^{-1}$ for 19Ti-HMS and these values are in a good agreement with data published previously for similar type of materials with lower content of Ti in matrix [37, 40]. Such high values of specific surface area together with type IV isotherms with capillary condensation step and H4 hysteresis loop indicate mesoporous character of solids (Fig. 3). Pore size distribution for all three matrices exhibits distribution of pore diameter in the range from 2 to 4 nm (see inset in the Fig. 3 and Tabel 1). S_{BET} of catalyst modified by vanadium is significantly lower, as is very often observed for impregnated catalysts [3, 10, 28]. Surface area loss ranges from ca. 25% for V-HMS sample to 44% for V-6Ti-HMS sample. This surface area loss is attributed in the literature to partial destruction of the framework [32] or rather by blocking of pores by oxide nanoclusters (in this case not detectable by XRD) because our previous works showed systematic surface degree with increasing vanadium content [3, 10, 32].

The IR spectra of powder supports and catalysts in KBr pellets before and after reaction are reported in the Figure 4 in the 1300–400 cm^{-1} range, where the skeletal vibrational modes occurs. The bands at 1228, 1091, 963, 798 and 470 cm^{-1} perceptible in all spectra are characteristic for the silica network. The broad feature at 1228 and 1091 cm^{-1} is assigned to inter-tetrahedral and intra-tetrahedral asymmetric stretch vibrations of T-O-T,

respectively. Bands at 798 and 470 cm^{-1} can be assigned to symmetric stretching modes of T-O-T vibration and T-O bending modes, respectively. Finally, the feature at 950 cm^{-1} can be assigned to two overlapping peaks of ν(Si-O-H) and ν(Ti-O-Si) vibration [1, 33, 44, 54]. In any case, no spectral feature of crystalline TiO_2 (anatase and/or rutile) with characteristic dominant broad band at 600-650 cm^{-1} [55-57] was detected in the spectra of KBr pellets of both Ti-HMS supports. This is another indication that titanium is relatively homogeneously incorporated into framework. All catalysts after reaction condition treatment have the same spectral characteristics as the fresh catalysts; no changes in the band intensity or occurrence of new band were detected. Therefore, it can be concluded that catalysts are stable under reaction conditions.

Thermal stability of supports was investigated by DTA in the temperature range from ambient temperature to 1200 °C (see Figure 5). DTA curves of all three supports exhibit weak endothermic process at about 130 °C, which is ascribed to removal of physisorbed molecules of water and long time drift of baseline caused by different values of thermal heat capacity of samples and α-Al_2O_3 standard referent respectively. No other process was detected for pure silica HMS support. On the contrary, exothermic processes are observed above 650 °C for Ti-HMS supports (peak maxima are at 750, 900 and 1040 °C for 19Ti-HMS and at 1050 and 1080 °C for 6Ti-HMS). These signals can be assigned to destruction of mesoporous titanosilicate framework and separation of SiO_2 and TiO_2 phase [55]. Similar behaviour was published by Morey [43] for material Ti-MCM-48 which is stable up to 800 °C. On the other hand some authors reported stability of titanium mesoporous silica materials even up to 1000 °C [58].

DR UV-vis spectra of both supports and vanadium catalysts under study are presented in Figure 6. All samples exhibit absorption bands in the range of photon energies from 3 to 6 eV attributed to ligand to metal charge-transfer (LMCT) transitions of the $O \rightarrow V^{+V}$ and/or $O \rightarrow Ti^{+IV}$ type. HMS support exhibits only very low intensity spectrum, whereas spectra of Ti-HMS supports exhibit very intense absorption bands with maxima at 4.29, 4.70 and 5.74 eV (289, 264 and 216 nm, respectively), which overlap absorption bands belonging to vanadium species in the spectra of vanadium catalysts. This is in a good agreement with spectra published previously for mesoporous titanosilicate support [27, 37, 40]. LMCT transitions are strongly influenced by the type and number of ligands surrounding the central metal ion in the first coordination sphere and, therefore, provide information on its local coordination environment. The absorption edge energy (E_g) of the spectra is usually employed

for this purpose [6, 59-60]. The values of E_g of all samples are listed in Table 1. Comparison of our Ti-HMS samples spectra with spectra of referent materials (TS-1 representing isolated titanium atoms surrounded by SiO_4 tetrahedra and rutile representing bulk Ti-O-Ti network) displayed in the $[F(R_\infty)\ h\nu]^2$ vs. $h\nu$ coordinates (see inset in Figure 6) led to conclusion that titanium in our samples is predominantly present in the form of isolated TiO_4 tetrahedra, because values of energy edges of our samples is 3.78 eV and 3.72 eV for 6Ti-HMS and 19Ti-HMS, respectively. These values are very close to the value of energy edge of TS-1 silicalite (E_g = 3.82 eV) whereas rutile/anatase exhibits lower energy edge (E_g = 3.11 eV) [40, 61]. Small differences in energy edge value of TS-1 and our materials (lower value of E_g) is probably due to small amount of titanium species coordinated in an octahedral coordination or Ti-O-Ti clustering in the framework, which are not detected by XRD [40, 62]. Presence of vanadium complexes in the sample leads to increase in intensity of spectra and slight red-shift of energy edges to the lower value. Energy edges of all vanadium catalysts fall to very narrow interval from 3.73 to 3.65 eV indicating very similar distribution of vanadium species. Based on the empirical correlation of these values with the structure of referent compounds and absorption edge energies of their UV-vis spectra (sodium ortho-vanadate Na_3VO_4 with E_g = 3.83 eV and meta-vanadate $NaVO_3$ E_g = 3.16 eV as compounds containing only isolated monomeric tetrahedral units and linearly polymerized tetrahedral units [47]) can be concluded that all vanadium species in our investigated catalysts are in tetrahedral coordination (no spectral signals under 3,16 eV). Unfortunately, we can not determine the amount of monomeric and polymeric species, as was published previously [3, 10]. Determination prevents overlapping absorption bands belonging to vanadium species by the intensive bands belonging to titanium. On the other hand we can say that most of species are in isolated or low-polymeric form.

H_2-TPR curves of VO_X catalysts are depicted in Figure 7 and values of onset temperature and temperature of reduction peak maxima are summarized in Table 1. It should be noted that parent supports exhibited no reduction peaks and therefore they are not reported here for the sake of brevity. TPR curves of all samples exhibit only one reduction peak in the temperature range from 400 to 800 °C. The overall hydrogen consumption corresponds to change of oxidation state during the reduction. The change of oxidation state varies from 1.6 to 2.1 of electrons per vanadium atom (see Table 1) indicating reduction from V^{+V} to V^{+III} or in some case partially only to V^{+IV}. Maximum of the reduction peak shifts to higher temperature with increasing titanium content. V-HMS catalysts exhibit reduction peak with

maximum at 562 °C, whereas maxima of reduction peaks of V-Ti-HMS catalysts are at 586 and 609 °C for V-6Ti-HMS and V-19Ti-HMS, respectively. In addition, the reduction peak becomes broader with increasing titanium content. However, it is contrary to investigation of redox behaviour of vanadium species on pure titanium oxide or pure silica support reported in the literature. Most authors present that vanadium complexes on TiO_2 are more reducible (reduction of vanadium on the TiO_2 proceed at a temperature about 100°C lower) than vanadium on silica support [63-64]. But we can see this behaviour only at V-titanosilicates where the support is prepared by impregnation of pure silica by titanium [28]. Reiche [64] who investigated V-titaniumsilicate aerogels prepared by direct synthesis and impregnated by vanadium showed the same results as in our work and this observation proves successful synthesis of titanosilicate with Ti-O-Si bonds. However, we must take into account that redox behaviour of supported vanadium species is very complex problem and can be affected by structural changes during heating of the sample, nature of vanadia complex (monomer/polymer/oxide) or nature of support and interaction of vanadia with support [3, 65-66]. In addition, we must take into account that only part of vanadia species is probably coordinated to surface in close vicinity of titanium. Shift of TPR onset to lower temperature with increasing vanadium content clearly indicates interaction of vanadium complexes with titanium (see Table 1).

3.2 *Catalytic tests of n-butane ODH*

Oxidative dehydrogenation of n-butane over investigated samples was studied at 460 °C. Main results for both prepared supports and vanadium impregnated catalysts are presented in Figure 8 and Table 2. The main reaction products identified in the reaction mixture were: 1-butene (1-C_4), *cis*- and *trans*-2-butene (*c*-C_4 and *t*-C_4), 1,3-butadiene (1,3-C_4), methane (C_1), ethane and ethene (C_2), propane and propene (C_3), carbon oxides (CO_X) and traces of acetaldehyde. The carbon balance was 98 ± 3 % in all catalytic tests and no coke deposit was observed on the catalysts. The activity of catalysts only slightly depended on the time-on-stream (TOS) and changes in conversion degree were less than 1 % during 10 hours.

All prepared supports exhibited measurable activity in the activation of n-butane. The catalytic activity of both titanosilicate matrices was significantly higher when compared to the pure silica material, and *ca.* 5% conversion degree of n-butane was obtained over these materials. The ability of titanosilicate matrix to activate alkanes was also reported in ODH of propane by TS-1 catalyst [67]. Because the activity of supports can not be neglected, it must

be taken into account in the evaluation of the activity of prepared vanadium based catalyst. The catalytic activity of obtained vanadium impregnated materials was higher for all catalysts than activity of pure support material. The highest change of catalytic activity was obtained for sample of V-19Ti-HMS for which the *n*-butane conversion increased from 6 to 17 % after VO_X impregnation.

The degree of *n*-butane conversion obtained over our samples did not exceed 20%, hence it can be assumed that the value of conversion is at first approximation proportional to the reaction rate. The summation of conversion values obtained on the Ti-HMS and V-HMS materials can be under this assumption taken as a proportional to hypothetic reaction rate occurring on the system of two independent active sites. These sum of conversion values on Ti-HMS and V-HMS material (in Figure 8 presented as hollow red circle point) are for both V-Ti-HMS materials lower than experimentally obtained values of conversion of *n*-butane. Therefore, some synergy effect can be observed. The V/TiO_2 based catalysts are reported [11, 27, 31-32, 68] as materials with significantly higher activity in partial oxidation or oxidative dehydrogenation of alkanes in comparison to V/SiO_2 based materials. Hence, the observed enhancement of catalytic activity over the mesoporous titanosilicate supported vanadium oxide catalysts is an evidence of the interaction of vanadium atoms with titanium oxide species on the surface of these materials.

The selectivity to sum of C_4-ODH products obtained over prepared samples of catalysts was below 50% and highest selectivity to these products (46%) was obtained over the sample V-HMS. Selectivity to C_4-ODH products was in all cases lower over pure matrices and the impregnation of vanadium increased the selectivity to ODH products and decreased the selectivity to products of *n*-butane cracking. The presence of titanium in catalysts slightly decreased the selectivity to C_4-ODH products, but the lowering of this value does not exceed 10 % for the sample V-6Ti-HMS. It can be seen that V-19Ti-HMS sample exhibited comparable selectivity to C_4-ODH products (44%) comparable to selectivity which was achieved on the sample V-HMS.

To the best of our knowledge, the only reported results on C_4-ODH over VO_X-titanosilicate catalysts were presented by Santacesaria et al. [11] who also published only small changes in selectivity to C_4-ODH products over VO_X-TiO_2/SiO_2 based catalyst in comparison to the VO_X/SiO_2 samples. The comparison of our results with data from this paper also clearly shows significant differences in distribution of individual C_4-ODH products. The

1,3-butadiene was the most abundant product in our C_4-ODH products over all vanadium containing catalysts with the selectivity *ca.* 20% and similar high selectivity to 1,3-butadiene was published previously [3] over the other set of V-HMS materials, whereas the Santacesaria *et. al.* [11] published nearly equimolar selectivity to 1-C_4, *t*-2-C_4 and *c*-2-C_4 with only a small amount of 1,3-C_4 (less than 12%) for catalysts with similar vanadium concentration. Moreover the similar distribution of C_4-ODH products which was obtained in mentioned paper was obtained also over both of our Ti-HMS supports. Differences in the selectivity to C_4-ODH products between catalysts cannot be ascribed to one simple effect, but more likely to the superposition of two effects. The significantly lower contact times were used in mentioned article, which is also indicated by the lower reported conversion values (less than 10%) compared to conversion values reached over our VO_X catalysts. It could be one effect which suppresses the occurrence of subsequent ODH reactions which can be a source of 1,3-butadiene. Nevertheless, solely this effect cannot explain the difference between the 1,3-C_4 selectivity over our Ti-HMS supports and VO_X-Ti-HMS catalysts. The higher selectivity to 1,3-butadiene over our VO_X containing catalysts in comparison to the Ti-HMS support materials is hence most likely caused by one-step subsequent ODH reaction of butenes occurring without the desorption to the gas phase, facilitated by the more acidic nature of VO_X active sites which prolongs the time of alkene retention on the surface as it was recently suggested [7, 69]

The productivity of C_4-ODH products over prepared vanadium containing catalysts is presented in Figure 9. It can be clearly seen that productivity to desired C_4-ODH products increases with increasing amount of titanium mesoporous support. When we compare the results obtained for vanadium catalysts impregnated on Ti-HMS support with our recently published data [3] it is evident that the presence of titanium in the mesoporous HMS matrix has significant promoting effect to the catalytic activity of V-Ti-HMS materials. The activity of V-19Ti-HMS catalyst at 460 °C is comparable with the activity of previously reported material I-VHMS-2.1 at 540 °C retaining the selectivity to C_4-ODH products, except for slightly higher selectivity to 1,3-butadiene. The improvement of activity of VO_X catalyst impregnated on mesoporous titanosilicate support hence offers the possibility to carry the reaction at lower temperature or to use catalysts with lower loading of vanadium.

4 Conclusion

Here presented results indicate successful one-pot synthesis of mesoporous titanosilicate with high titanium content (up to 19 wt. %) isomorphously incorporated into

framework. No method of characterization detected signals attributable to bulk TiO_2 phase either for neither fresh materials nor catalysts after reaction conditions (460°C for at least 10 h). These materials seem to be promising supports for vanadium oxide-based catalysts allowing their good dispersion. Advanced properties of these materials were demonstrated in C_4-ODH reaction. Productivity to desired C_4-ODH products was four times higher for titanosilicate materials compared with silica-based V-HMS materials and reached value up to 280 g of C_4 alkenes per 1 kg of catalyst per hour.

Acknowledgement

The authors thank to project of the Czech Science Foundation No. P106/10/0196 for financial support.

References

[1] A. Comite, A. Sorrentino, G. Capannelli, M. Di Serio, R. Tesser and E. Santacesaria, J. Mol. Catal. A-Chem., 198 (2003) 151.
[2] L.M. Madeira and M.F. Portela, Catal. Rev.-Sci. Eng., 44 (2002) 247.
[3] M. Setnicka, R. Bulanek, L. Capek and P. Cicmanec, J. Mol. Catal. A-Chem., 344 (2011) 1.
[4] H.H. Kung, Advances in Catalysis, Vol. 40, Academic Press Inc, San Diego, 1994, p. 1.
[5] B.M. Weckhuysen and D.E. Keller, Catal. Today, 78 (2003) 25.
[6] H.J. Tian, E.I. Ross and I.E. Wachs, J. Phys. Chem. B, 110 (2006) 9593.
[7] T. Blasco and J.M.L. Nieto, Appl. Catal. A, 157 (1997) 117.
[8] E.A. Mamedov and V.C. Corberan, Appl. Catal. A, 127 (1995) 1.
[9] R. Bulanek, A. Kaluzova, M. Setnicka, A. Zukal, P. Cicmanec and J. Mayerova, Catal. Today, 179 (2012) 149.
[10] R. Bulánek, P. Čičmanec, H. Sheng-Yang, P. Knotek, L. Čapek and M. Setnička, Appl. Catal. A, (2012).
[11] E. Santacesaria, M. Cozzolino, M. Di Serio, A.M. Venezia and R. Tesser, Appl. Catal. A, 270 (2004) 177.
[12] S. Albonetti, F. Cavani and F. Trifiro, Catal. Rev.-Sci. Eng., 38 (1996) 413.
[13] R.M. Martin-Aranda and J. Cejka, Top. Catal., 53 (2010) 141.
[14] F. Cavani, J. Chem. Technol. Biotechnol., 85 (2010) 1175.
[15] A.A. Teixeira-Neto, L. Marchese and H.O. Pastore, Quim. Nova, 32 (2009) 463.
[16] I.E. Wachs and B.M. Weckhuysen, Appl. Catal. A, 157 (1997) 67.
[17] E.V. Kondratenko, M. Cherian, M. Baerns, D.S. Su, R. Schloegl, X. Wang and I.E. Wachs, J. Catal., 234 (2005) 131.
[18] Q.H. Zhang, Y. Wang, Y. Ohishi, T. Shishido and K. Takehira, J. Catal., 202 (2001) 308.
[19] W. Liu, S.Y. Lai, H.X. Dai, S.J. Wang, H.Z. Sun and C.T. Au, Catal. Lett., 113 (2007) 147.
[20] P. Gruene, T. Wolfram, K. Pelzer, R. Schlogl and A. Trunschke, Catal. Today, 157 (2010) 137.
[21] Y.M. Liu, Y. Cao, N. Yi, W.L. Feng, W.L. Dai, S.R. Yan, H.Y. He and K.N. Fan, J. Catal., 224 (2004) 417.
[22] F. Ying, J.H. Li, C.J. Huang, W.Z. Weng and H.L. Wan, Catal. Lett., 115 (2007) 137.

[23] L. Capek, R. Bulanek, J. Adam, L. Smolakova, H. Sheng-Yang and P. Cicmanec, Catal. Today, 141 (2009) 282.
[24] P. Knotek, L. Capek, R. Bulanek and J. Adam, Top. Catal., 45 (2007) 51.
[25] K. Cassiers, T. Linssen, M. Mathieu, M. Benjelloun, K. Schrijnemakers, P. Van Der Voort, P. Cool and E.F. Vansant, Chem. Mater., 14 (2002) 2317.
[26] M. Kruk, M. Jaroniec and A. Sayari, Microporous Mater., 9 (1997) 173.
[27] N. Hamilton, T. Wolfram, G. Tzolova Muller, M. Havecker, J. Krohnert, C. Carrero, R. Schomacker, A. Trunschke and R. Schlogl, Catalysis Science & Technology, (2012).
[28] O. Ovsitser, M. Cherian, A. Bruckner and E.V. Kondratenko, J. Catal., 265 (2009) 8.
[29] E. Kondratenko, M. Cherian and M. Baerns, Catal. Today, 112 (2006) 60.
[30] A. Dinse, B. Frank, C. Hess, D. Habel and R. Schomacker, J. Mol. Catal. A-Chem., 289 (2008) 28.
[31] D. Shee and G. Deo, Catal. Lett., 124 (2008) 340.
[32] J.H. Kwak, J.E. Herrera, J.Z. Hu, Y. Wang and C.H.F. Peden, Appl. Catal. A, 300 (2006) 109.
[33] A. Zhang, Z. Li, Z. Li, Y. Shen and Y. Zhu, Appl. Surf. Sci., 254 (2008) 6298.
[34] W. Zhang, B.S. Zhang, T. Wolfram, L.D. Shao, R. Schlogl and D.S. Su, J. Phys. Chem. C, 115 (2011) 20550.
[35] M.A. Bañares, X. Gao, J.L.G. Fierro and I.E. Wachs, in S.T.O.A.M.G. R.K. Grasselli and J.E. Lyons (Editors), Studies in Surface Science and Catalysis, Vol. 110, Elsevier, 1997, p. 295.
[36] F. Bérubé, F. Kleitz and S. Kaliaguine, J. Mater. Sci., 44 (2009) 6727.
[37] A. Tuel, Microporous Mesoporous Mat., 27 (1999) 151.
[38] Y. Chen, Y. Huang, J. Xiu, X. Han and X. Bao, Appl. Catal. A, 273 (2004) 185.
[39] R.S. Araújo, D.C.S. Azevedo, E. Rodríguez-Castellón, A. Jiménez-López and C.L. Cavalcante Jr, J. Mol. Catal. A-Chem., 281 (2008) 154.
[40] W. Zhang, M. Fröba, J. Wang, P.T. Tanev, J. Wong and T.J. Pinnavaia, J. Am. Chem. Soc., 118 (1996) 9164.
[41] S. Gontier and A. Tuel, Zeolites, 15 (1995) 601.
[42] T. Blasco, A. Corma, M.T. Navarro and J.P. Pariente, J. Catal., 156 (1995) 65.
[43] M. Morey, A. Davidson and G. Stucky, Microporous Mater., 6 (1996) 99.
[44] M. Nandi and A. Bhaumik, Chemical Engineering Science, 61 (2006) 4373.
[45] P.T. Tanev and T.J. Pinnavaia, Science, 267 (1995) 865.
[46] M. Pouzar, T. Kratochvil, L. Capek, L. Smolakova, T. Cernohorsky, A. Krejcova and L. Hromadko, Talanta, 83 (2011) 1659.
[47] R. Bulanek, L. Capek, M. Setnicka and P. Cicmanec, J. Phys. Chem. C, 115 (2011) 12430.
[48] L. Capek, J. Adam, T. Grygar, R. Bulanek, L. Vradman, G. Kosova-Kucerova, P. Cicmanec and P. Knotek, Appl. Catal. A, 342 (2008) 99.
[49] P. Kubelka and F.Z. Munk, Tech. Phys., 12 (1931) 593.
[50] Y. Liu, K. Murata, M. Inaba and N. Mimura, Appl. Catal. A, 309 (2006) 91.
[51] C. Chen, Q.H. Zhang, J. Gao, W. Zhang and J. Xu, J. Nanosci. Nanotechnol., 9 (2009) 1589.
[52] S.A. Karakoulia, K.S. Triantafyllidis and A.A. Lemonidou, Microporous Mesoporous Mat., 110 (2008) 157.
[53] J. Santamaria-Gonzalez, J. Luque-Zambrana, J. Merida-Robles, P. Maireles-Torres, E. Rodriguez-Castellon and A. Jimenez-Lopez, Catal. Lett., 68 (2000) 67.
[54] G.W. Wallidge, R. Anderson, G. Mountjoy, D.M. Pickup, P. Gunawidjaja, R.J. Newport and M.E. Smith, J. Mater. Sci., 39 (2004) 6743.

[55] Y. Djaoued, S. Badilescu, P.V. Ashrit, D. Bersani, P.P. Lottici and J. Robichaud, J. Sol-Gel Sci. Technol., 24 (2002) 255.
[56] M. Ocana, V. Fornes, J.V.G. Ramos and C.J. Serna, J. Solid State Chem., 75 (1988) 364.
[57] P.M. Kumar, S. Badrinarayanan and M. Sastry, Thin Solid Films, 358 (2000) 122.
[58] M. Chatterjee, H. Hayashi and N. Saito, Microporous Mesoporous Mat., 57 (2003) 143.
[59] X.T. Gao and I.E. Wachs, J. Phys. Chem. B, 104 (2000) 1261.
[60] J. Tauc, Amorphous and Liquid Semiconductors, Plenum Press, London, 1974.
[61] C. Li, G. Xiong, Q. Xin, J.K. Liu, P.L. Ying, Z.C. Feng, J. Li, W.B. Yang, Y.Z. Wang, G.R. Wang, X.Y. Liu, M. Lin, X.Q. Wang and E.Z. Min, Angew. Chem.-Int. Edit., 38 (1999) 2220.
[62] W.H. Zhang, J.Q. Lu, B. Han, M.J. Li, J.H. Xiu, P.L. Ying and C. Li, Chem. Mater., 14 (2002) 3413.
[63] A. Sorrentino, S. Rega, D. Sannino, A. Magliano, P. Ciambelli and E. Santacesaria, Appl. Catal. A, 209 (2001) 45.
[64] M.A. Reiche, E. Ortelli and A. Baiker, Appl. Catal. B-Environ., 23 (1999) 187.
[65] B.E. Handy, A. Baiker, M. Schraml-Marth and A. Wokaun, J. Catal., 133 (1992) 1.
[66] F. Arena, F. Frusteri, G. Martra, S. Coluccia and A. Parmaliana, J. Chem. Soc.-Faraday. Trans., 93 (1997) 3849.
[67] W. Schuster, J.P.M. Niederer and W.F. Hoelderich, Appl. Catal. A, 209 (2001) 131.
[68] I.E. Wachs, J.M. Jehng, G. Deo, B.M. Weckhuysen, V.V. Guliants, J.B. Benziger and S. Sundaresan, J. Catal., 170 (1997) 75.
[69] L.C. Marcu, L. Sandulescu, Y. Schuurman and J.M.M. Millet, Appl. Catal. A, 334 (2008) 207.

Table 1
Chemical composition and results of physico-chemical characterization of investigated materials

Sample	$Ti_{(matrix)}$[a], wt.%	V[a], wt.%	S_{BET}, m^2g^{-1}	V_P[b], $cm^3\ g^{-1}$	D_{ME}[c], nm	T_{onset}[c], °C	T_{max}[c], °C	Δe[f]	ε_0, eV
HMS	0.00	0.0	**880**	**0.560**	2.4 - 3.1	—	—	—	—
V-HMS	0.00	1.5	**650**	—	—	397	562	2.1	3.73
6Ti-HMS	6.0	0.0	**890**	**0.532**	2.6 - 3.2	—	—	—	3.78
V-6Ti-HMS	6.0	1.5	**690**	—	—	376	586	2	3.66
19Ti-HMS	12.0	0.0	**800**	**0.495**	2.4 - 3.0	—	—	—	3.72
V-19Ti-HMS	12.0	1.5	**770**	—	—	376	609	1.6	3.65

[a] Titanium resp. vanadium content determined by XRF method (error: ±0.2 wt.%)

[b] V_P total pore volume determined at $p/p_0 = 0.97$

[c] D_{ME} mesopore diameter determined by NLDFT

[d] Onset temperature of H_2-TPR profile

[e] Position of maxima of H_2-TPR profile

[f] Average change of oxidation state during H_2-TPR experiment

[g] Energy of absorption edge determined by Tauc's method [60]

Table 2

Results of catalytic tests for bare supports and support with impregnated vanadium at 460 °C (m_{cat} = 400mg, $C_4H_{10}/O_2/He$ = 10/10/80 vol.%, total flow rate of 100 cm^3 min^{-1})

Sample	Conv., %	Selectivity							Yield, %	Productivity[c]
	C_4H_{10}	1-C_4	*c*-C_4	*t*-C_4	1,3-C_4	C_1-C_3[a]	CO_x	∑C_4.[b]	∑C_4	∑C_4
HMS	1	10	6	2	18	25	39	**36**	0.4	0.01
V-HMS	4	17	7	3	19	8	45	**46**	2.3	0.08
6Ti-HMS	5	8	7	10	4	4	67	**28**	1.5	0.06
V-6Ti-HMS	14	8	7	3	20	2	61	**37**	5.0	0.18
19Ti-HMS	6	10	9	13	5	4	59	**37**	2.1	0.08
V-19Ti-HMS	17	9	8	4	23	2	53	**44**	7.7	0.28

[a] C_1-C_3 = sum of C_1-C_3 hydrocarbons and acetaldehyde

[b] ∑C_4 = sum of C_4 alkene selectivity, yield or productivity, resp.

[c] Productivity = g_{prod} g_{cat}^{-1} h^{-1}

List of figure captions

Figure 1 - SEM images of mesoporous HMS and Ti-HMS supports.

Figure 2 – (A) Low-angle diffraction patterns for parent supports. (B) X-ray diffraction patterns for parent supports and supports after impregnation by vanadium (XRD patterns were offset for clarity).

Figure 3 - Nitrogen adsorption isotherms of bare supports (isotherms were offset for clarity). Inset: Pore size distribution of bare supports determined by DFT method for cylindrical pores and metal oxide surface.

Figure 4 - FT-IR spectra of KBr pellets of supports and supports after impregnation by vanadium (spectra were offset for clarity).

Figure 5 - Thermal analysis pattern of HMS and Ti-HMS supports (curves were offset for clarity).

Figure 6 - Diffuse reflectance UV-vis spectra of diluted and dehydrated supports and supports after impregnation by vanadium.

Figure 7 - H_2-TPR patterns of V-HMS and V-Ti-HMS samples (curves were offset for clarity).

Figure 8 - The conversion (full red circle and line), hypothetic conversion (hollow red circle point) and selectivity (stacked bar) of bare supports and support with impregnated vanadium in ODH of *n*-butane at 460°C. (For interpretation of the references to color in this figure legend, the reader is referred to the web version of the article.)

Figure 9 - Productivity to C_4 dehydrogenation products in *n*-butane ODH over V-HMS and V-Ti-HMS catalysts.

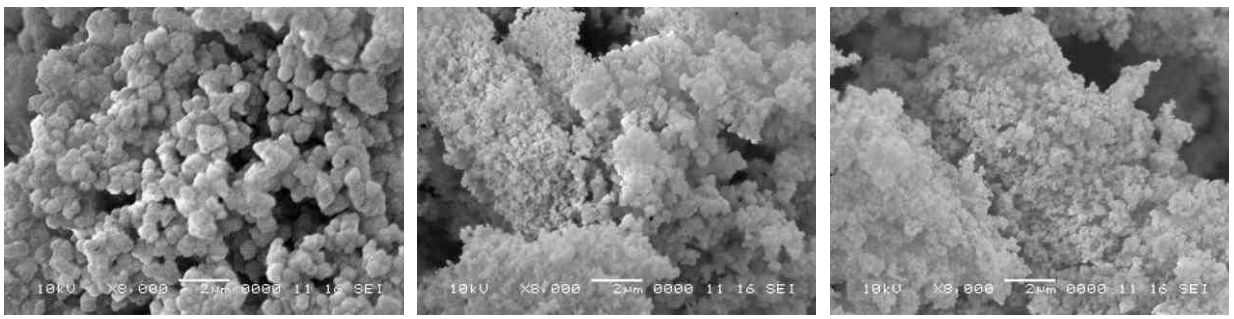

HMS 6Ti-HMS 19Ti-HMS

Figure 1

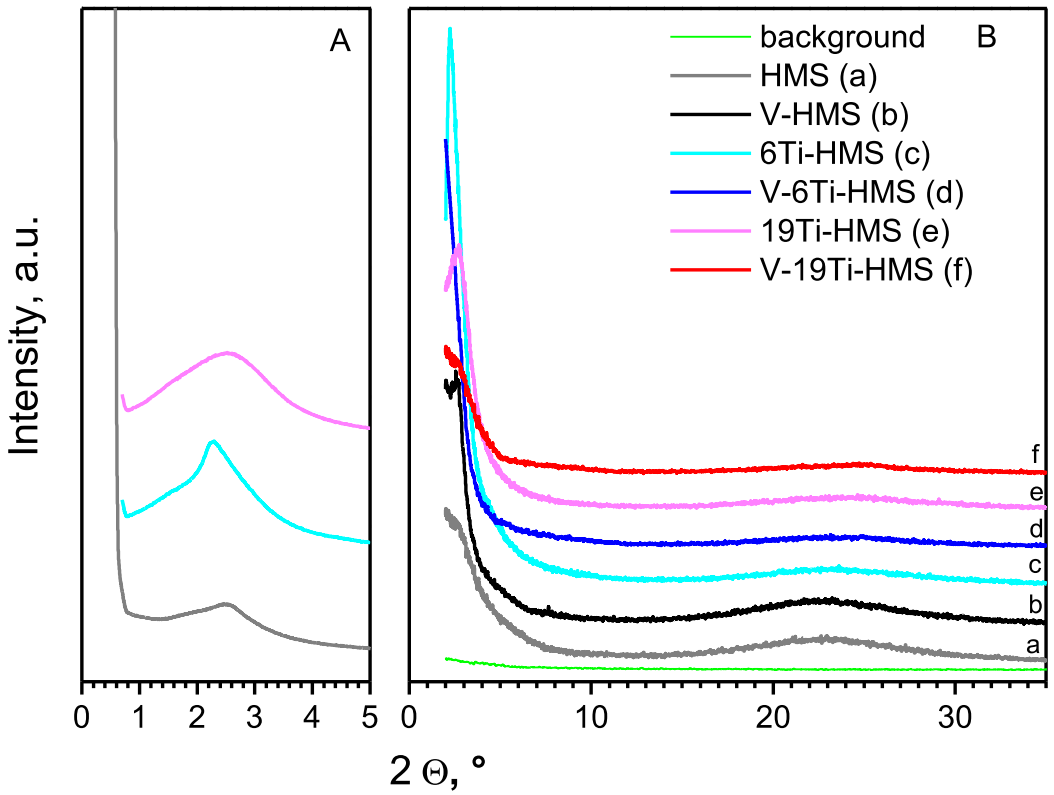
A
B
background
HMS (a)
V-HMS (b)
6Ti-HMS (c)
V-6Ti-HMS (d)
19Ti-HMS (e)
V-19Ti-HMS (f)
Intensity, a.u.
2 Θ, °
0
1
2
3
4
5
10
20
30
a
b
c
d
e
f

Figure 2

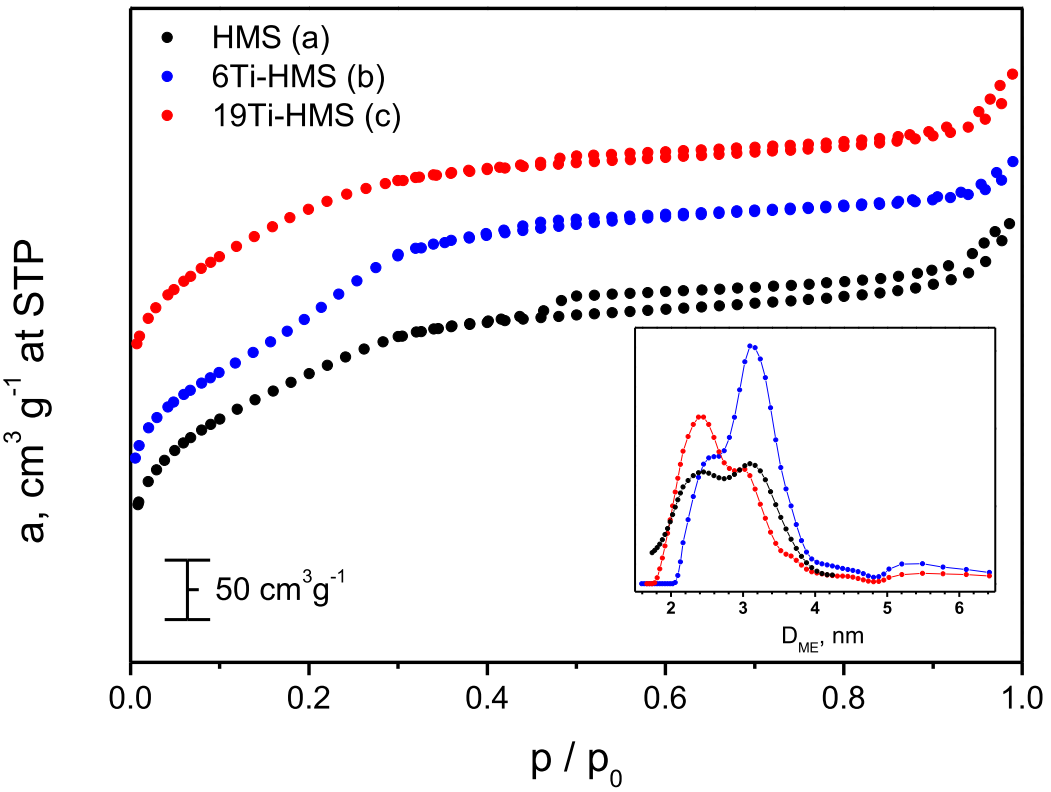
HMS (a)
6Ti-HMS (b)
19Ti-HMS (c)
a, cm3 g-1 at STP
50 cm3g-1
0.0
0.2
0.4
0.6
0.8
1.0
p / p0
2
3
4
5
6
DME, nm

Figure 3

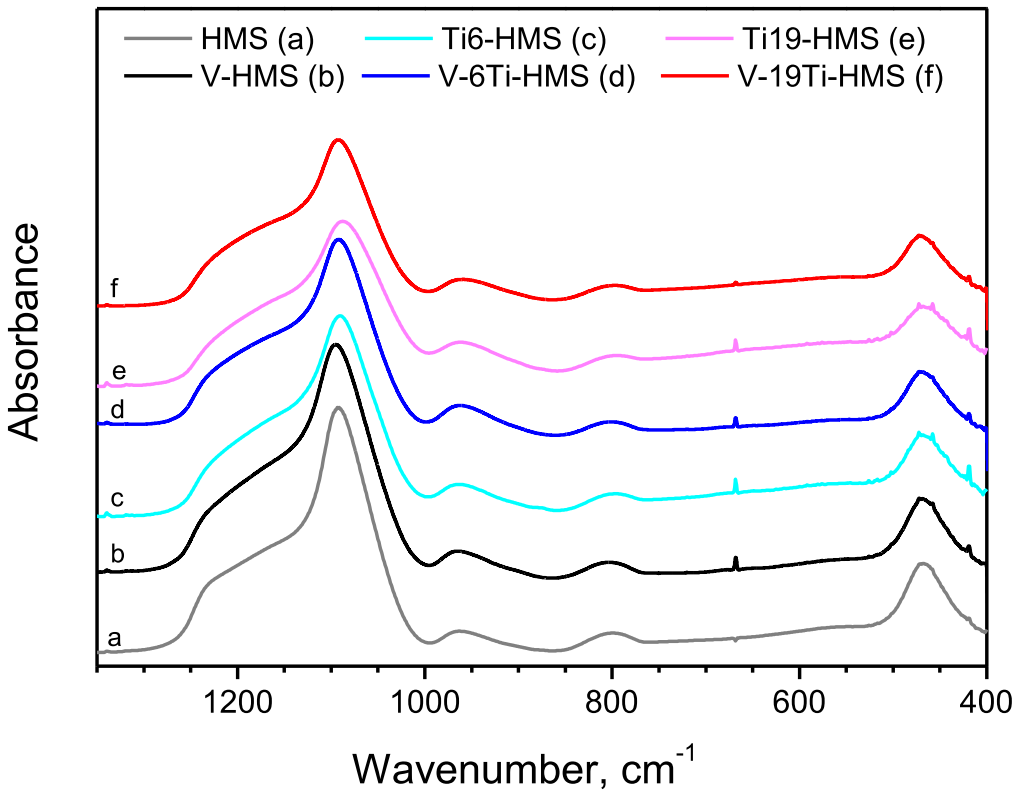
HMS (a)
Ti6-HMS (c)
Ti19-HMS (e)
V-HMS (b)
V-6Ti-HMS (d)
V-19Ti-HMS (f)
Absorbance
f
e
d
c
b
a
1200
1000
800
600
400
Wavenumber, cm-1

Figure 4

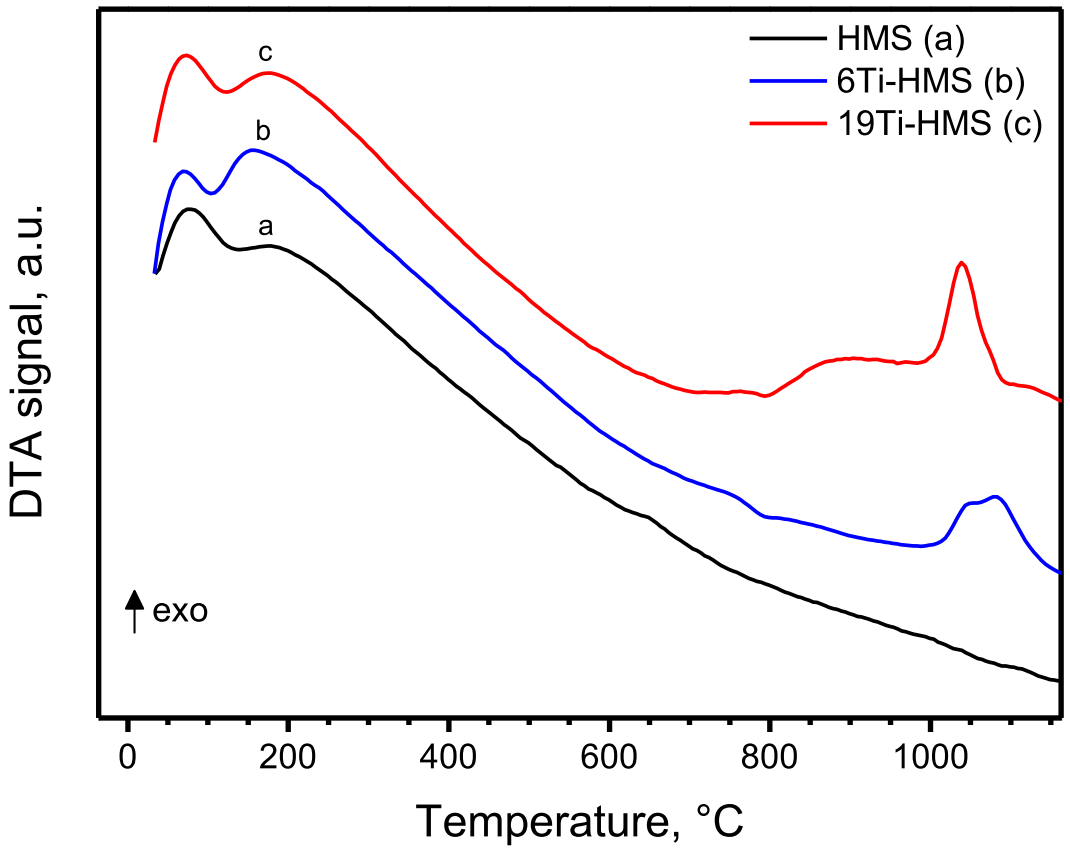
HMS (a)
6Ti-HMS (b)
19Ti-HMS (c)
c
b
a
exo
DTA signal, a.u.
0
200
400
600
800
1000
Temperature, °C

Figure 5

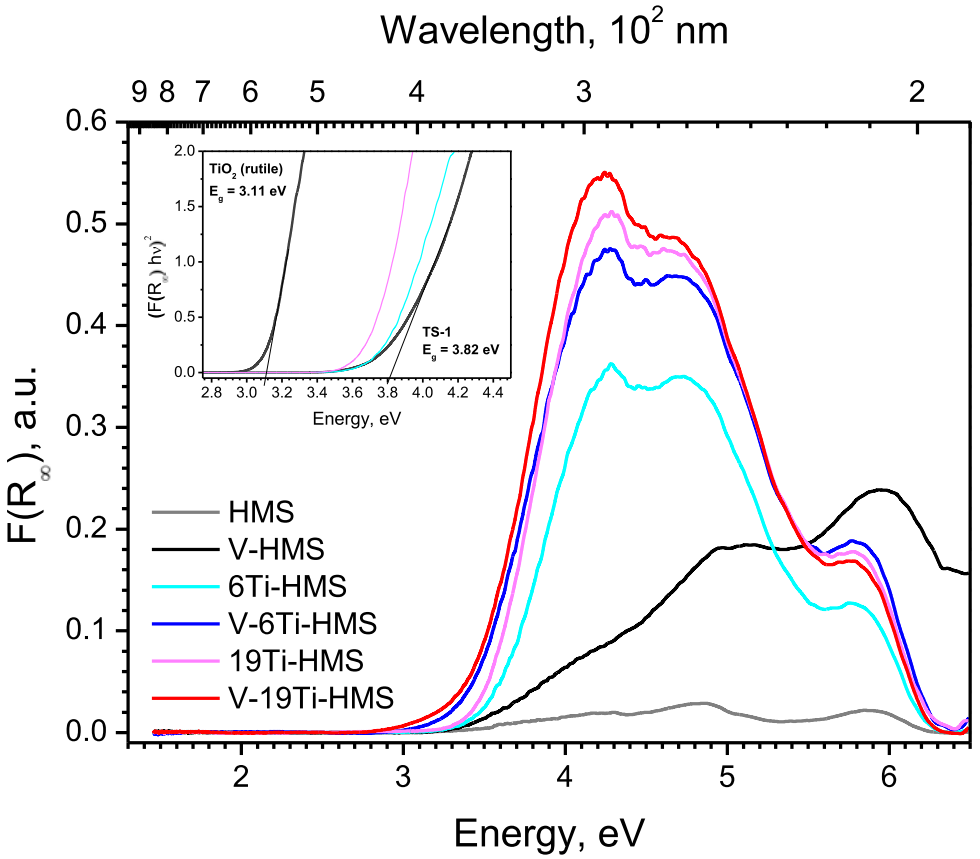
Wavelength, 10^2 nm
9 8 7 6 5 4 3 2
F(R∞), a.u.
Energy, eV
HMS
V-HMS
6Ti-HMS
V-6Ti-HMS
19Ti-HMS
V-19Ti-HMS
TiO2 (rutile)
Eg = 3.11 eV
TS-1
Eg = 3.82 eV
(F(R∞) hν)^2
Energy, eV

Figure 6

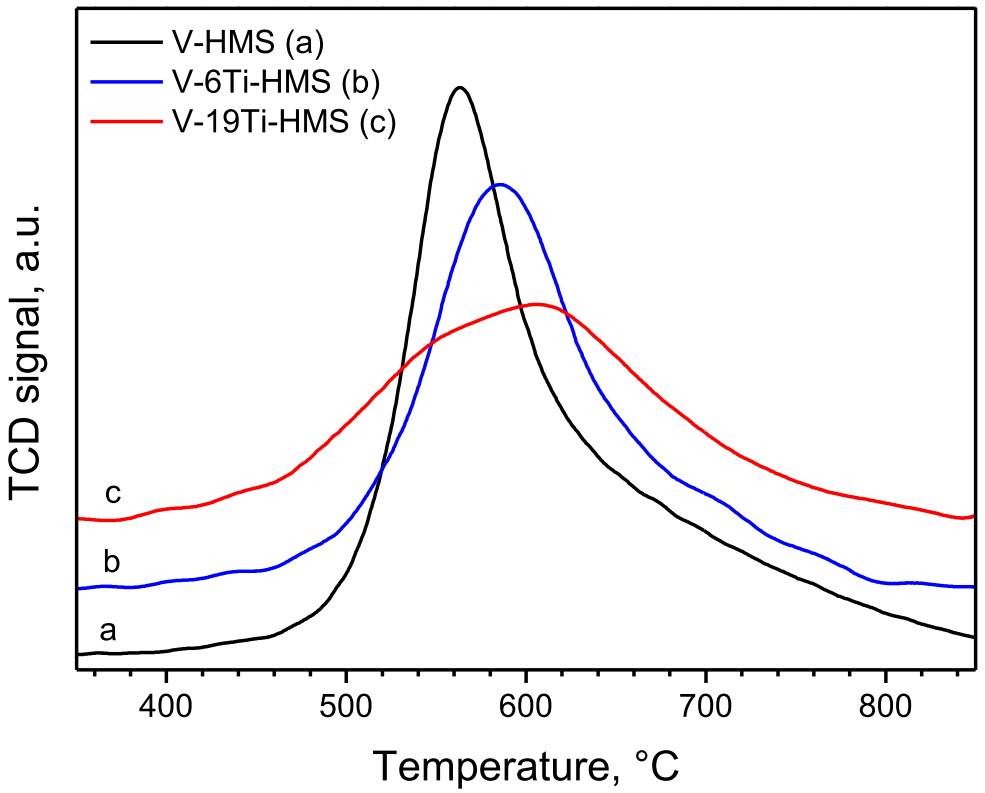
V-HMS (a)
V-6Ti-HMS (b)
V-19Ti-HMS (c)
TCD signal, a.u.
c
b
a
400
500
600
700
800
Temperature, °C

Figure 7

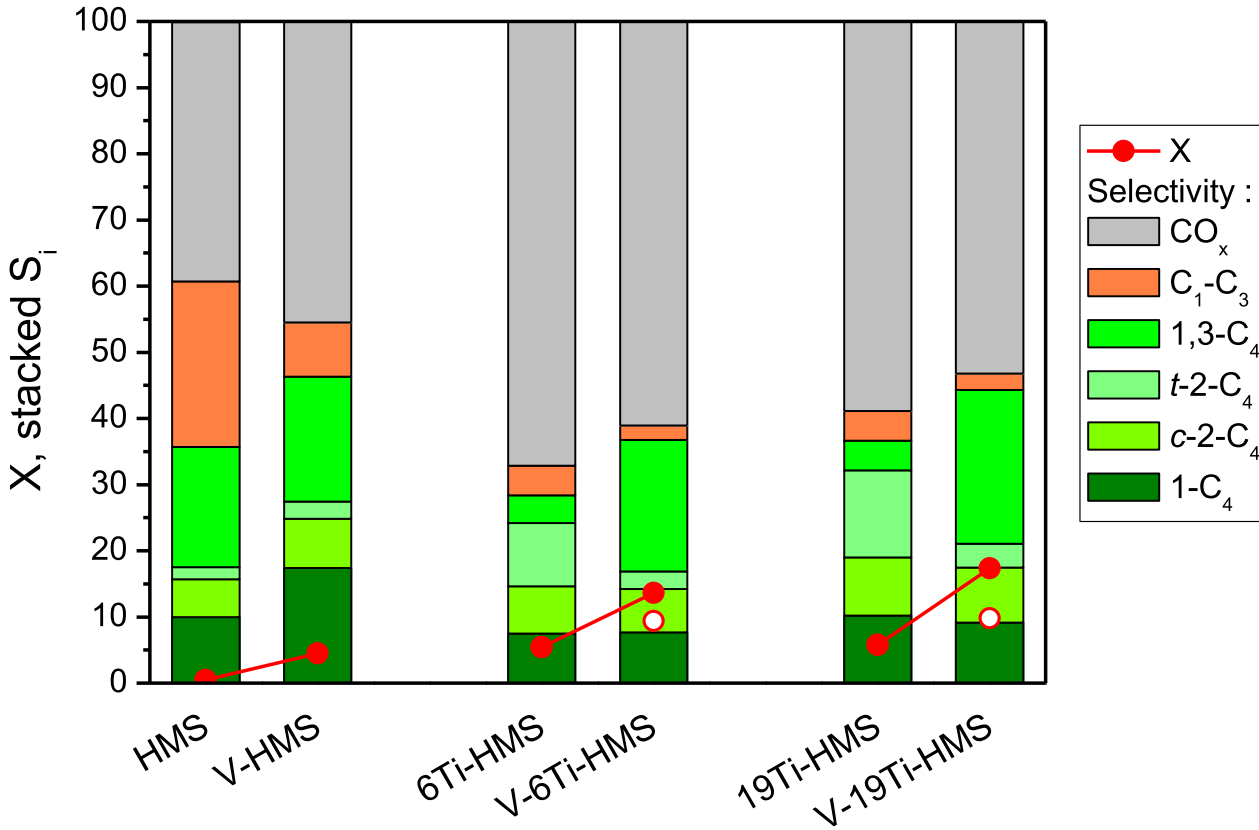
X, stacked S_i
100
90
80
70
60
50
40
30
20
10
0
HMS
V-HMS
6Ti-HMS
V-6Ti-HMS
19Ti-HMS
V-19Ti-HMS
X
Selectivity :
CO_x
C_1-C_3
1,3-C_4
t-2-C_4
c-2-C_4
1-C_4

Figure 8

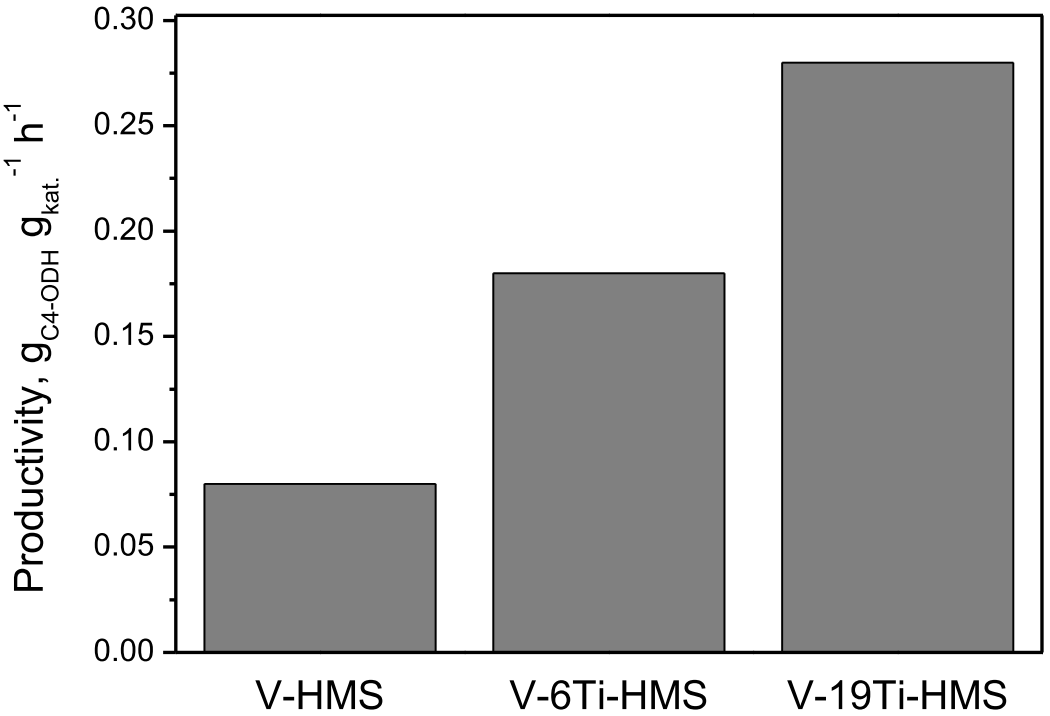
Productivity, $g_{C4\text{-}ODH}$ $g_{kat.}^{-1}$ h^{-1}
0.30
0.25
0.20
0.15
0.10
0.05
0.00
V-HMS
V-6Ti-HMS
V-19Ti-HMS

Figure 9